Model Studies of Prestressed Rigid Pavements for Airfields

PAUL F. CARLTON, Chief of Research Branch, and
RUTH M. BEHRMANN, Research Mathematician;
Ohio River Division Laboratories, Corps of Engineers, U.S. Army

● GROSS WEIGHTS of current and proposed military aircraft have reached such proportions that as much as 30 in. of plain concrete may be required to provide an adequate design for heavy-duty airfield pavements. The search for an improved method of constructing such heavy-duty pavements has led to the consideration of prestressing rigid pavements; that is, subjecting rigid pavements to compressive stresses of sufficient magnitude to reduce significantly the critical tensile stresses normally produced by service loadings. Little data, however, are available upon which to base a rational method of design for prestressed pavements, since the use of prestressing in the United States has been confined almost entirely to structures other than airfield and highway pavements. In 1953, the Corps of Engineers initiated studies to determine the feasibility of utilizing prestressed pavements for military airfields and to develop procedures for the design and evaluation of such pavements. These studies are being made as a part of the Rigid Pavement Investigational Program conducted by the Ohio River Division Laboratories.

In one phase of the ORDL program, small scale models have been used to provide basic information concerning the behavior of prestressed rigid pavements under various conditions of loading. This paper presents the significant information obtained from the model tests completed to date. As such, this paper should be considered a progress report rather than a final report of the model tests.

TEST PROGRAM

In the model, prototype conditions were simulated through the use of small prestressed gypsum cement slabs placed on an artificial subgrade of natural rubber. Static loads were applied to the slabs by means of single footprints of various sizes. Whenever possible, comparable tests were made on plain slabs having no prestressing and on slabs having unequal amounts of longitudinal and transverse prestressing so that the performance of these types of pavements could be compared with pavements having equal longitudinal and transverse prestressing. In the testing completed to date, the following types of observations and measurements have been made: (a) crack patterns and crack development for various conditions of loading, (b) deflections measured for interior and edge loadings for elastic and elasto-plastic conditions in the slabs, (c) maximum strains and strain distribution measured for interior and edge loadings within the elastic limit of the slabs, and (d) ultimate load-carrying capacity of the slabs for various conditions of loading. A general view of the model and the auxiliary equipment is shown in Figure 1.

DESIGN OF THE MODEL

In order that Westergaard's theoretical analyses of rigid pavement behavior could be applied to certain phases of these studies, it was necessary to consider the simulation of some of the basic assumptions inherent in his analyses. The theory assumes that the materials comprising the slab and subgrade are homogeneous and isotropic, that the slab is of uniform thickness, and that the slab is large enough to act as though infinite in horizontal extent. Since Westergaard's analyses are valid only where critical stresses in the slab and subgrade remain within their respective elastic limits, no correlation between the theory and the model existed for conditions of inelastic action in the slabs.

The model slabs were cast from Hydrocal gypsum cement. Each slab was 16.6-in. square and approximately 0.20-in. thick. For this thickness, the radius of relative

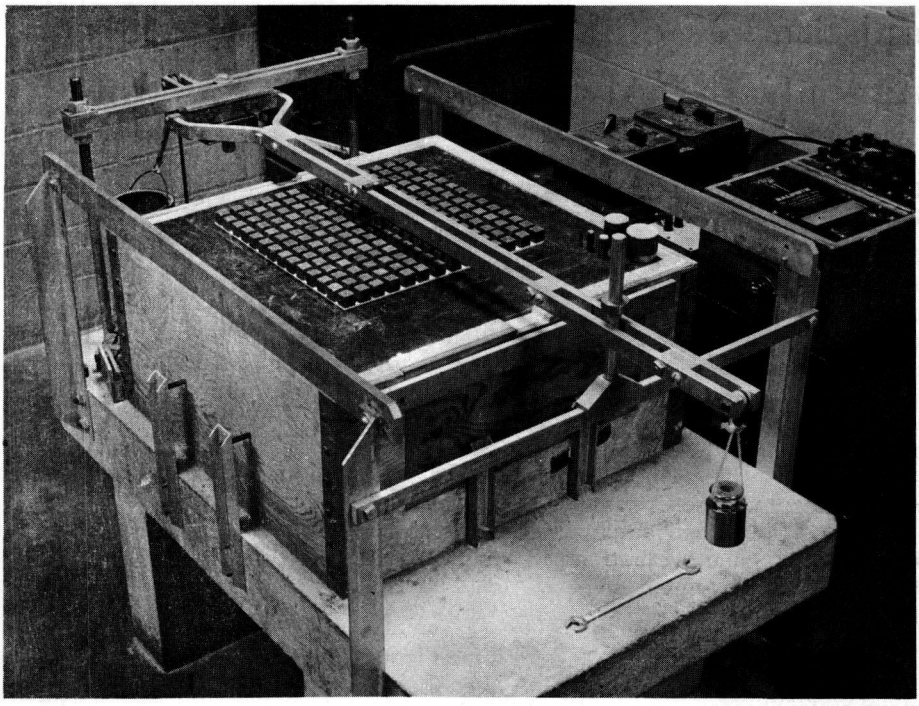

Figure 1. Model table with prestressed slab in place for testing.

Figure 2. Combination tensioning frame and casting form used in constructing the test slabs. Anchorage device for maintaining wire tension is shown in the foreground.

stiffness, l, of each slab was 2.4-in. making the horizontal dimensions of each slab 7 l by 7 l. For all practical purposes, slabs of this size act as though infinite in extent as required by the Westergaard analyses. To increase the effective mass of the slabs and thereby insure intimate contact at the interface between the slabs and the subgrade, a layer of $\frac{3}{4}$-in. lead cubes was distributed uniformly over the surface of each test slab.

For the hydrocal, values of the various physical properties used in the analysis of the model tests were determined to be:

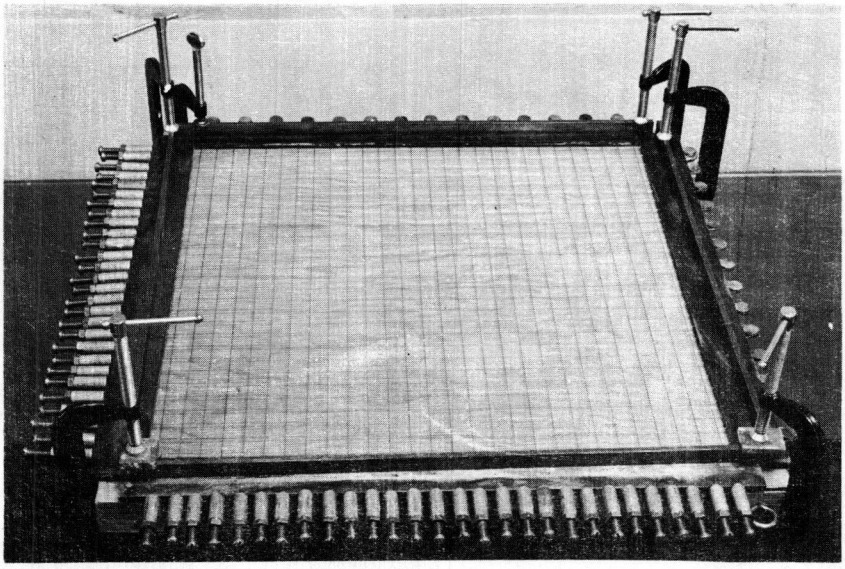

Figure 3. Longitudinal and transverse wires in place ready for the final tensioning.

Modulus of elasticity - 1.50×10^6 psi,

Poisson's ratio - 0.225,

Flexural strength - 940 psi,

Compressive strength - 3,200 psi.

A complete description of the above model techniques as applied to the study of plain concrete pavements has been given in (1) and (2).

Prestressing

The slabs were prestressed longitudinally and transversely by tensioned music wires positioned at the neutral axis of each slab. The decision to place the stressing wires at the mid-depth of the slabs was based largely on the fact that for testing within the elastic limit of the slabs, the presence of the wires should have no effect on altering the stiffness of the slabs. Wire spacing, wire diameter and the range of loads applied to the wires used in the model were chosen arbitrarily to provide a range of conditions of prestressing similar to that anticipated for prototype pavements. Although prestressing in the prototype may be effected by tensioning the stressing tendons either before or after the placing and curing of the concrete, only the "pre-tensioning" technique was used in the construction of the model slabs.

Inasmuch as the bond developed between the Hydrocal and the music wire was an important factor in determining the maximum amount of prestressing that could be applied to the slabs, pull-out tests were made on various lengths of wire embedded in Hydrocal beams one inch square in cross-section. From these tests, it was concluded

TABLE 1

SUMMARY OF DESIGN VARIATIONS IN THE PRESTRESSED SLABS

Slab Number	Slab Thickness in.	Wire Spacing, in.		Prestressing, lb/in.^{2}		Radius of Relative Stiffness, in.		Remarks
		Long.	Trans.	Long.	Trans.	Interior k = 35	Edge k = 65	
1-X	0.204	0.6	0.6	150	150	2.8360	2.4296	Preliminary-Hydrostone
2-X	0.201	0.6	0.6	600	600	2.3509	2.0140	Cracked diagonally in releasing
1	0.202	0.6	0.6	600	600	2.3596	2.0215	
2	0.200	0.6	0.6	600	600	2.3422	2.0066	
3	0.206	0.6	0.6	600	600	2.3946	2.0515	
4	0.202	0.6	0.6	600	600	2.3596	2.0215	
5	0.206	1.2	1.2	360	360	2.3946	2.0515	
6	0.204	1.2	1.2	360	360	2.3771	2.0365	Two small edge cracks in releasing
7	0.214	1.2	0.6	360	600	2.4641	2.1110	Three wires failed in bond-replacement slab being constructed
8	0.205	0.6	0.6[a]	600	360	2.3860	2.0441	
9	0.206	0.6	None	600	0	2.3946	2.0515	
10	0.204	0.6	0.6	600	600	2.3771	2.0365	
11	0.208	1.2	1.2	360	360	2.4121	2.0664	
12	0.208	0.6[b]	0.6	360	600	2.4121	2.0664	
13	0.201	0.6	0.6	600	600	2.3509	2.0140	
14	0.208	0.6	0.6	600	600	2.4121	2.0664	

[a] 45 lb per wire — all others 75 lb per wire

[b] 0.14-in. diameter wire — all others 0.20-in. diameter wire

Slabs constructed of Hydrocal (except No. 1-X), $E = 1.5 \times 10^6$, $\mu = 0.225$

TABLE 2

SUMMARY OF PRESTRESSED STRAINS, TEST SLAB NO. 12

Gage No.	Measured Strain x 10^6 in./in.					Average 48 hr
	0 hr	6 hr	24 hr	30 hr	48 hr	
1	52	62	134	111	123	
5	158	146	166	182	167	
6	36	50	98	113	124	138
2	243	256	295	294	314	
3	305	331	357	361	373	
4	345	437	460	466	469	385
7	200	222	225	239	231	
8	206	223	242	251	248	240

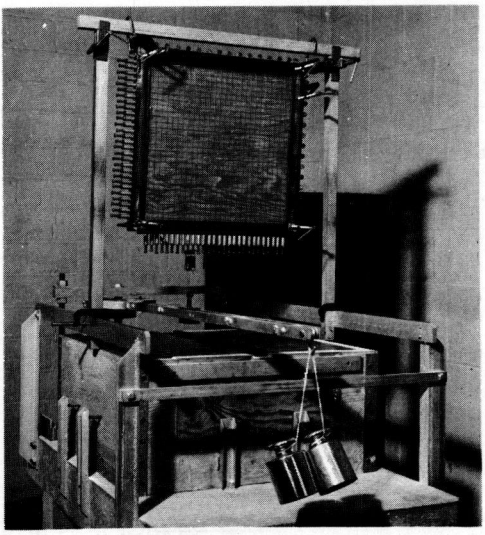

Figure 4. Arrangement for applying the desired tension to the prestressing wires. Tension developed in the wires by means of the reaction beam is maintained by tightening the locknut on each anchorage device.

that the individual wires in the model slabs could be pretensioned as much as 75 and 50 lb for 0.020- and 0.014-in. diameter wire, respectively, without danger of exceeding the bond strength.

Most of the model slabs constructed to date have been stressed with 0.020-in. diameter (No. 8) wire which had an average tensile strength of 366,000 psi. The maximum loading of 75 lb produced an initial tensile stress of 239,000 psi or approximately 65 percent of the ultimate tensile strength of the wire. For a uniform wire spacing of 0.6-in. center-to-center and a pretensioning load of 75 lb per wire, a maximum prestress of 600 psi was developed in the model slabs.

Subgrade

In the model, simulation of the prototype subgrade was made by using a 24-in. square block of natural rubber 12-in. in depth. This block of rubber was supported rigidly by a concrete table and the sides were restrained laterally by a rigid casting. Since, in terms of l, this subgrade was 5 l deep, it acted as though infinite in depth as required by the Westergaard analyses. The modulus of subgrade reaction, k, of the rubber was determined to be 65 lb per cu in. for edge loadings and 35 lb per cu in. for interior loadings.

Loading

Service loadings on the prototype were simulated in the model through the use of various sizes of circular and elliptical footprints. The footprints were loaded statically by means of the reaction beam as shown in Figure 1. For the tests reported herein, only single-wheel loadings were investigated.

Instrumentation

Instrumentation used in the testing was limited to that necessary for observing strains and deflection developed in the model slabs. Strain measurements were made using

TABLE 3

COMPARISON OF FAILURE LOADS FOR PLAIN AND PRESTRESSED SLABS LOADED AT THE INTERIOR

Footprint Radius (in.)	Load (lb)			
	Plain		Prestressed 600 psi x 600 psi	
	First Crack	Ultimate Failure	First Crack	Ultimate Failure
0.2	30	74	42	95
0.3	36	72	50	125
0.4	40	86	59	150
0.5	44	90	66	180
0.75	54	104	88	228

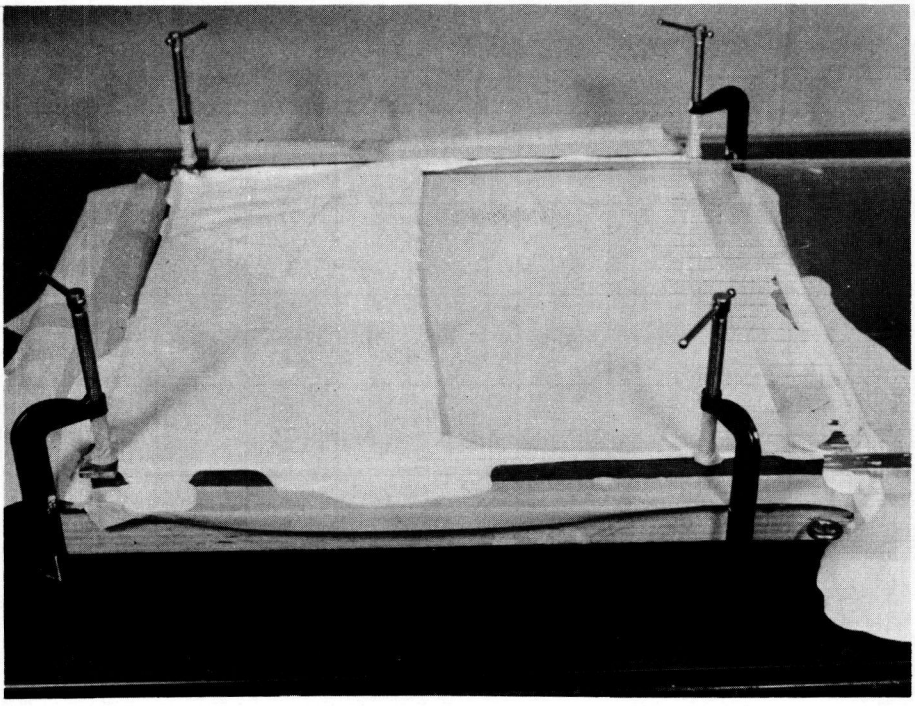

Figure 5. Striking off the top surface of the slab using a $\frac{1}{2}$-in. thick glass plate.

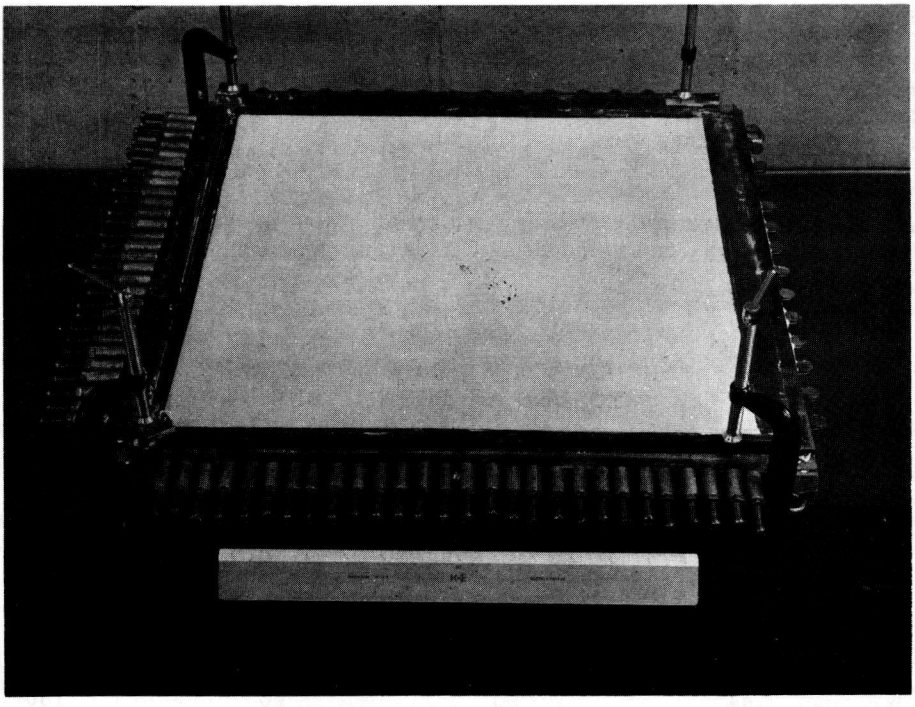

Figure 6. Test slab approximately 45 min after casting. Prestressing applied and casting frame removed after a minimum curing period of 7 days.

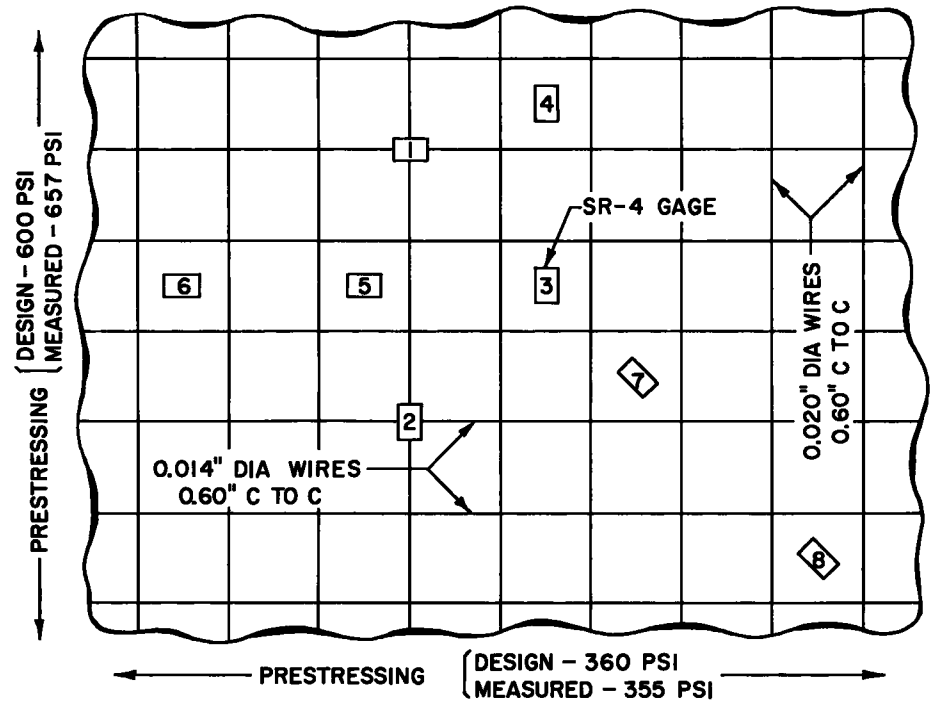

Figure 7. Arrangement of SR-4 strain gages for measuring effective prestress - Slab No. 12.

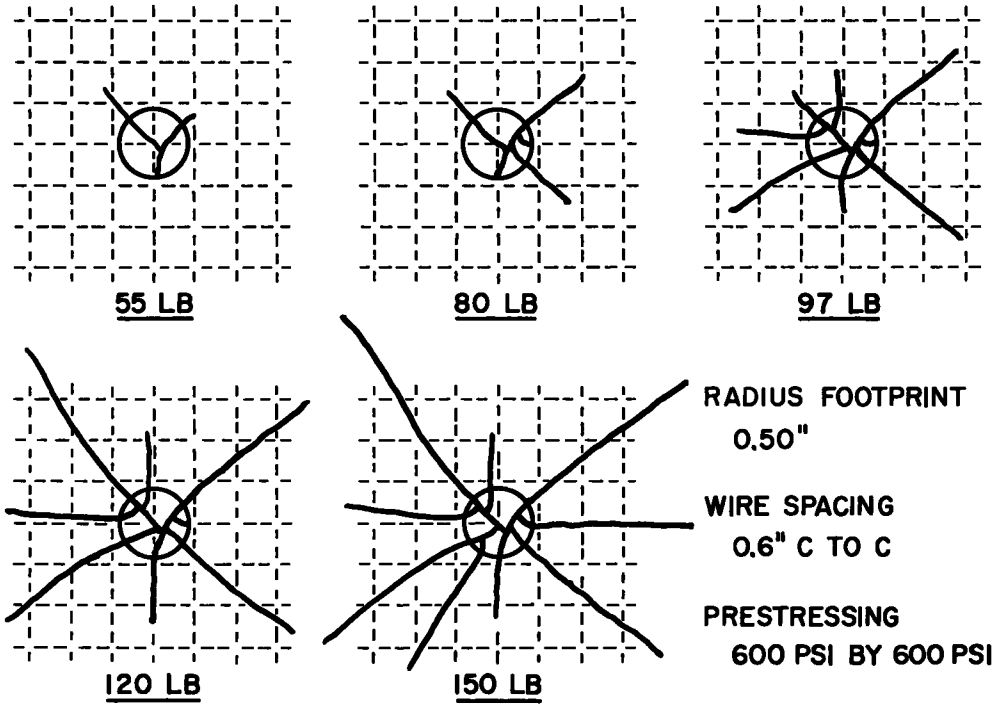

Figure 8. Progression of cracking for interior loading - Slab No. 1.

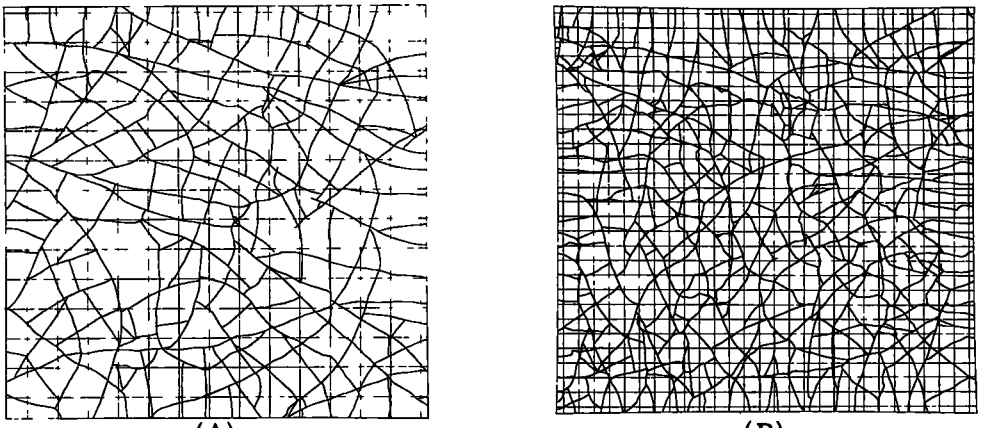

(A) (B)

Figure 9. (A) Test slab No. 5, prestressing 360 psi by 360 psi, wire spacing 1.20 in. by 1.20 in., 75-lb load; (B) Test slab No. 10, prestressing 600 psi by 600 psi, wire spacing 0.60 in. by 0.60 in., 90-lb load. Crack patterns developed in the bottom side of two test slabs. Slabs loaded using an 0.75-in. radius footprint applied at 1-in. intervals over the entire area of the slab.

Type A-7, SR-4 gages and a Baldwin SR-4 Control Box. Dial gages reading direct to 0.0001-in. were used in measuring all deflections.

CONSTRUCTION OF THE MODEL SLABS

The model slabs were cast in a form constructed of four 18- by 1.5- by 0.20-in. steel bars clamped to a base consisting of a glass plate cemented to a 1½-in. thick piece of plywood. The steel side forms were fabricated with 0.031-in. diameter holes at mid-depth and spaced 0.6-in. center-to-center. The stressing wires were strung through these holes so that all wires in the same direction were in the same plane and the neutral axis of the slab was at the point of tangency of the two layers of wires. Each wire was secured by an anchoring device which permitted adjustment of the tension in the wire to any desired value. Details of the stressing frame, anchorage devices and sequence of placing the wires are shown in Figures 2 and 3.

The required tension in each stressing wire was obtained by using the reaction beam of the model table to apply the proper load, as illustrated in Figure 4. Correct tension was maintained in the wire by tightening the lock nut on the anchorage device. To compensate for the deflection of the steel frame which resulted from tensioning the wires, it was necessary to repeat the application of the load on each wire. Normally, two checks on the tension in the wires were made prior to casting the slab.

Following the final tensioning of the wires, the slab was cast from Hydrocal gypsum cement having a water-cement ratio of 54 percent. The strike-off of the top side of the slab was made with a ½-in. thick glass plate as shown in Figure 5. The use of glass plates to form the top and bottom sides of the test slabs produced uniformly thick slabs having smooth plane surfaces.

Approximately 45 min after the slab was cast, the strike-off glass was removed and the excess Hydrocal cleaned from the side forms and wire anchorages. A completed slab approximately one hour after casting is shown in Figure 6. The slab was then allowed to cure in air under controlled temperature (73 deg F.) and humidity (50 percent) for a minimum period of seven days. Following the curing period, the prestressing was applied to the slab by releasing the wires from the anchorages and removing the slab from the form. For those slabs were SR-4 strain gages were used to check the effective prestressing developed in the slab, the gages were cemented to the top surface of the cured slab and allowed to air-dry 48 hr before the application of the prestressing.

A total of 16 test slabs have been constructed to date for this study. Several variations in prestressing have been incorporated in these slabs to provide data on the relative effects of equal longitudinal and transverse prestressing, unequal longitudinal and

transverse prestressing, and prestressing in one direction only. These variations were accomplished by altering the spacing and diameter of the stressing wires, and by changing the tension in the wires. Table 1 is a summary of the physical characteristics and conditions of prestressing for each slab.

TEST RESULTS

Check on Prestressing

For several slabs an attempt was made to determine the net amount of prestress developed by the method of construction employed. This was done by mounting SR-4 strain gages on the top surface of the slab prior to the release of the wires. The arrangement of the strain gages for Slab No. 12, as shown in Figure 7, was typical for all such testing.

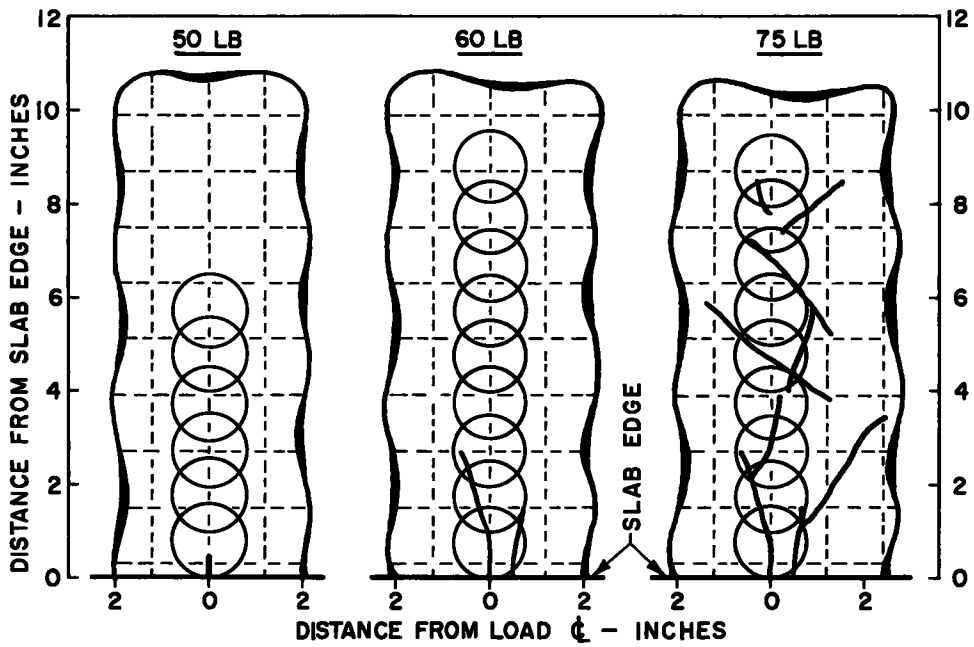

Figure 10. Development of cracking for simulation of wheel-load moving from a free edge to interior — Slab No. 6, 0.75-in. radius footprint.

Strains were read immediately following the release of the stressing wires and again at various intervals for a period of 48 hr thereafter. The prestressing was computed on the basis of the average strains obtained from each group of parallel gages. The results of these measurements indicated that the full amount of prestressing was not realized immediately, but reached a maximum approximately 36 to 48 hr after application. The initial prestress immediately after releasing the wires was generally 75 percent of the ultimate amount, with 95 percent of the ultimate being reached within 24 hr after releasing. Typical strain data, as obtained from Slab No. 12, are shown in Table 2. Based on the average strains measured 48 hr after releasing, the prestressing was 355 psi longitudinally and 657 psi transversely as compared to design values of 360 and 600 psi, respectively.

Crack Patterns

One of the attributes of testing with a small scale model is the fact that the slab can be removed from the model table for examination after being subjected to various loadings. This made it possible to observe the development of crack patterns in the bottom side of the slab as loadings were carried beyond the elastic limit.

In order to study the progression of cracking for a single position of the load in the interior of a slab, the load was applied in increasingly greater amounts until the initial crack occurred. The slab was then removed from the model table and the location and extent of the crack noted. After replacing the slab on the subgrade, the load was increased further until additional cracking occurred. Typical of the results obtained using this procedure are the crack patterns shown in Figure 8 for loadings on an 0.5-in. radius footprint positioned near the center of Slab No. 1.

As can be seen in Figure 8, the cracking is predominantly radial in nature and originates under the center of the loaded area. Although the 150 lb load represented approximately 85 percent of the ultimate load for Slab No. 1, at no time were any cracks observed in the top side of the slab. Testing of this type was repeated on other slabs having wire spacings and prestressing different from that in Slab No. 1 without significant differences in the crack patterns formed. Similarly, it was observed that the pattern of cracking was not affected by centering the load over a wire intersection or between the wires.

Somewhat different crack patterns were formed in Slabs Nos. 5 and 10 as the result of applying a load large enough to cause cracking at all points over the surface of each slab. These patterns, shown in Figure 9, were developed by loading each slab with an 0.75-in. radius footprint at one-inch intervals over the entire slab area. Loading of this nature more nearly simulates the loading experienced in the prototype than does the idealized loading shown in Figure 8. A comparison of the crack patterns for Slabs Nos. 5 and 10 reveals a closer spacing of cracks for a closer spacing of stressing wires. The exact effect of the difference in wire spacing was obscured to a degree by the fact

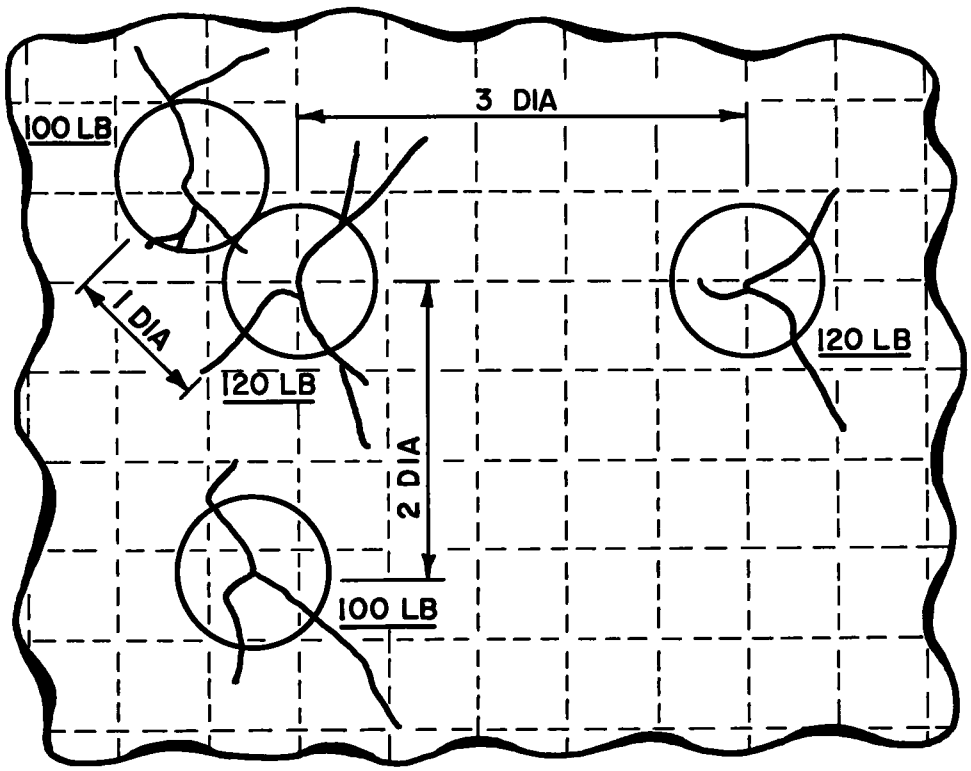

Figure 11. Formation of independent plastic hinges for interior loading - Slab No. 14.

that the greater prestress in Slab No. 10 required a heavier load to produce cracking. Again, none of the cracking was visible on the top side of either slab.

In an attempt to obtain information pertaining to the relative load-carrying ability of a prestressed slab subjected to edge loading and interior loading, Slab No. 6 was loaded in a manner as shown in Figure 10. Using an 0.75-in. radius footprint, the slab was loaded initially with the footprint tangent to a free edge and then moved at intervals of one inch to the center of the slab. This procedure was repeated for three loadings, beginning with the load producing the initial edge crack. The data presented in Figure 10

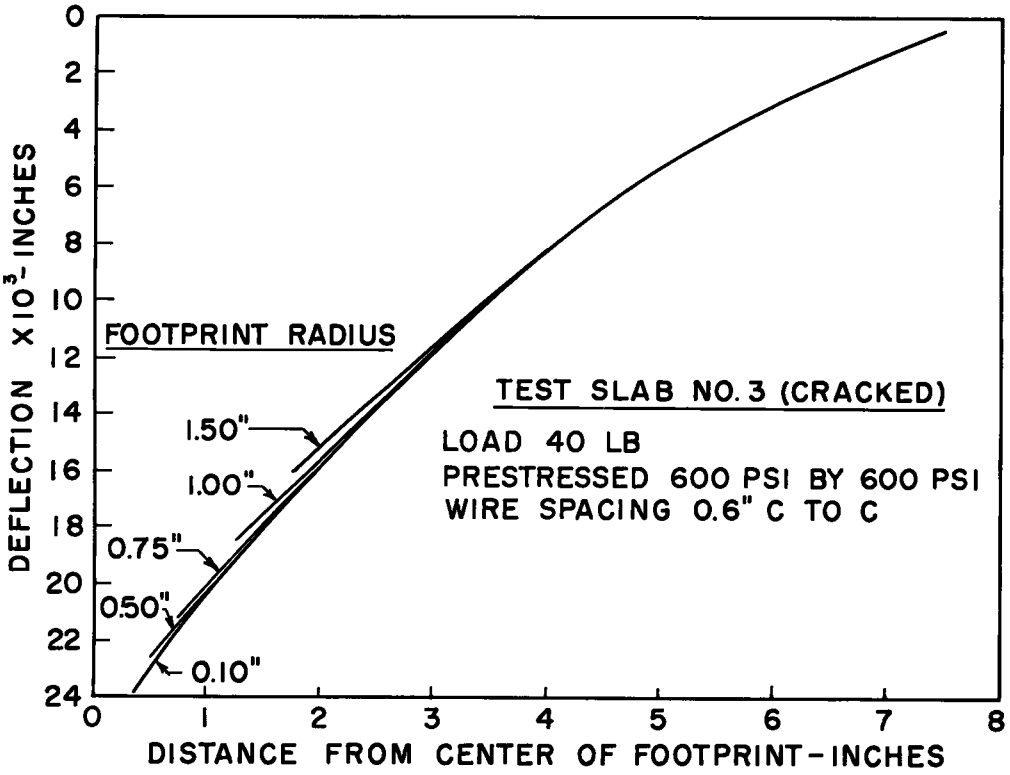

Figure 12. Effect of footprint size on deflections for interior loading of cracked slab.

clearly indicates the inherently greater load-carrying ability of the slab when subjected to interior loadings as compared to loadings at a free edge.

Basic information regarding the formation of plastic hinges within a prestressed slab was obtained from tests on Slab No. 14. Using an 0.5-in. radius footprint, loadings were made to determine the minimum distance between load applications that would result in the formation of independent plastic hinges. With the footprint positioned near the center of the slab, a load was applied until the initial crack was formed in the bottom side of the slab. The footprint was then moved, in order, to alternate positions three, two, one, and three-quarters diameters distant from the original load position. These alternate load positions were selected so that the cracking resulting from the original load was tangential, insofar as possible, to them. At each alternate position of the footprint, the slab was loaded until new cracking occurred. The relative positioning of the footprint for loadings producing independent cracking and the cracks developed at each of these points of loading are shown in Figure 11. Since independent cracks were formed in all cases except when the loads were spaced three-quarters of a diameter apart, it was indicated by these tests that independent plastic hinges could be developed in a prestressed slab for loadings spaced one or more diameters apart, center-to-center.

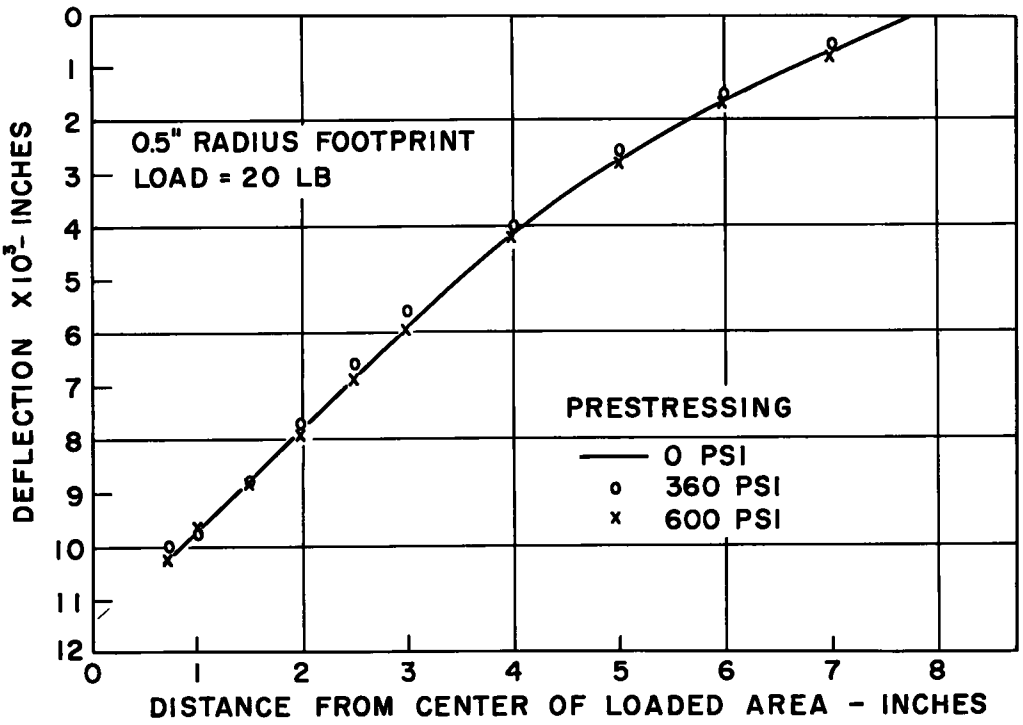

Figure 13. Effect of different prestressing on deflections within the elastic range.

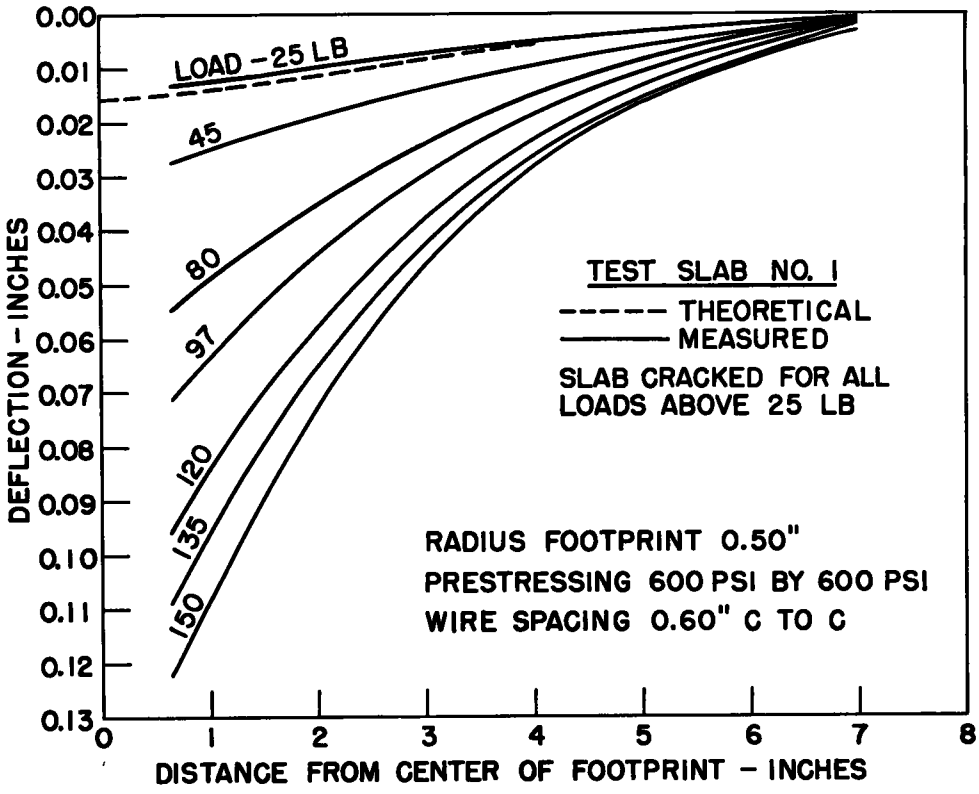

Figure 14. Deflection curves for interior loadings.

Deflections

Due to the construction of the footprints and the method of loading used, it was not possible to obtain deflection measurements within the contact area of the load. Therefore, all deflection data are for measurements at the footprint edge and beyond.

Deflection measurements were made to study the effects of such variables as: footprint size, prestressing, load, and degree of cracking. The results of tests to observe the effect of footprint size on slab deflections for a partially cracked slab are shown in Figure 12. Footprints ranging in radius from 0.10- to 1.50-in. were positioned in the center of a cracked area approximately 2½-in. in diameter in the interior portion of Slab No. 3. Each footprint was loaded to 40 lb and deflections were measured from the edge of the footprint to the edge of the slab. As can be seen from Figure 12, footprint size had little or no effect on deflections beyond the loaded area. Since these deflections are in substantial agreement with Westergaard's analyses, it was indicated that the presence of the cracking had little influence on the deflections for this loading.

In order to determine the effect of the magnitude of prestressing on slab deflections, tests were made on three slabs having different ratios of longitudinal to transverse prestressing as follows: 0 to 600 psi, 360 to 600 psi, and 600 to 600 psi, respectively. Identical loadings of 20 lb on an 0.5-in. radius footprint were made on each slab. The deflections shown in Figure 13 are those measured in the longitudinal direction and indicate that, within the elastic range, the variation in prestressing had no influence.

In conjunction with the study of crack pattern development for loading near the center of Slab No. 1, slab deflection measurements were made for comparison with the progression of cracking with increasing load. These deflections are shown in Figure 14. For the 25-lb load, the critical stresses in the slab did not exceed the elastic limit of the slab and the measured deflections were in good agreement with those computed on the basis of the Westergaard analyses. The deflections measured for loads greater

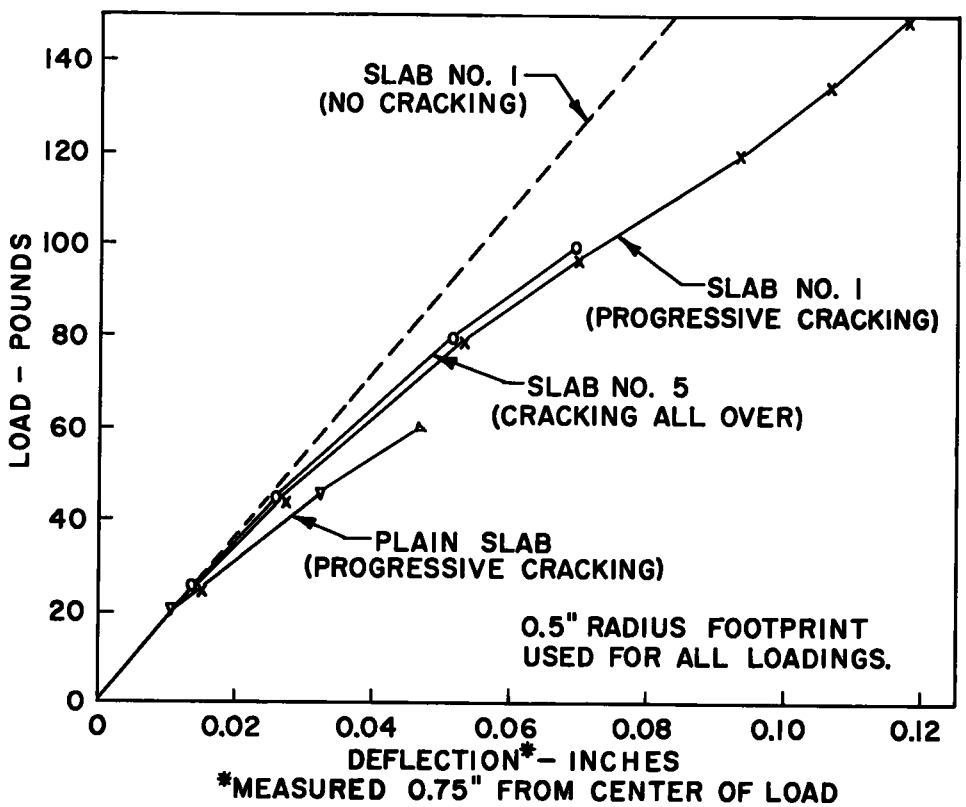

Figure 15. Deflections for interior loadings on plain and prestressed slabs.

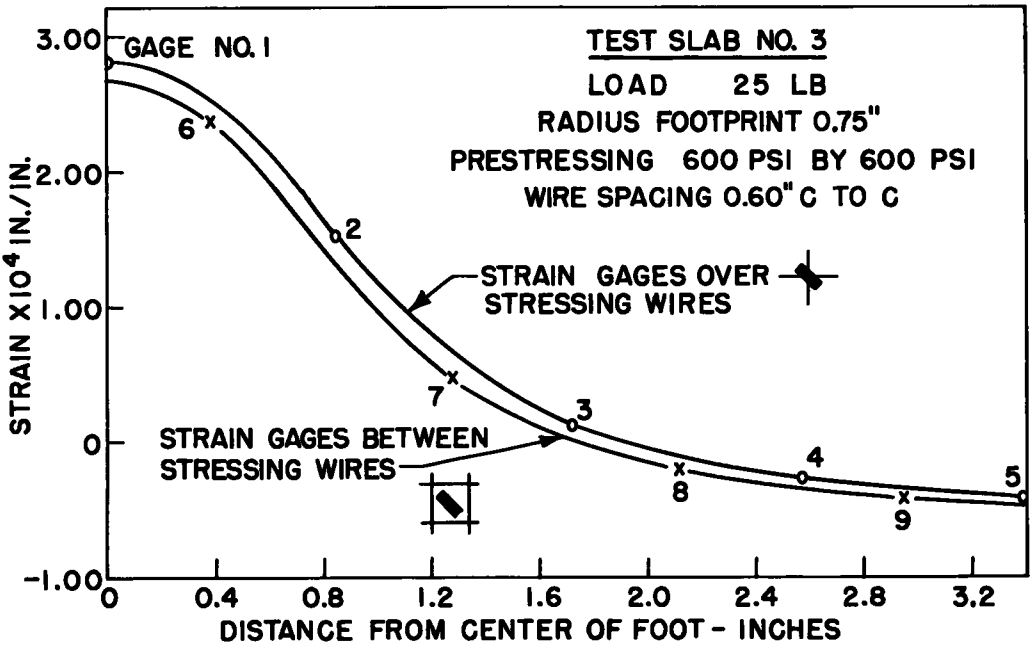

Figure 16. Effect of strain gage orientation on measured strains.

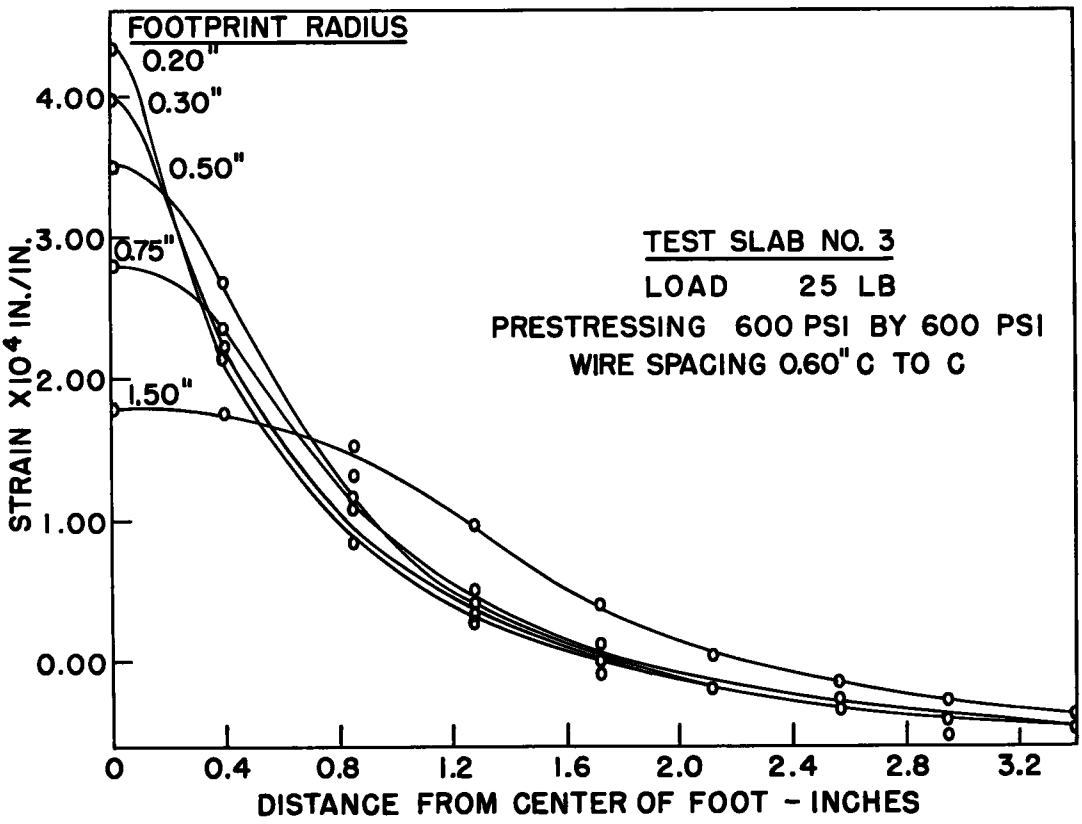

Figure 17. Effect of footprint size on strain distribution for interior loadings within the elastic range.

than 25 lb were for the progressively greater degree of cracking associated with each loading. Based on maximum deflections obtained from extrapolation of the curves plotted in Figure 14, it appears that the degree of cracking observed for a load of 150 lb (see Fig. 8) permits approximately 50 percent greater deflections than would be experienced if no cracks were present in the slab.

Figure 15 is a comparison of deflection versus load curves for two prestressed slabs and one plain slab, each loaded near the center with an 0.5-in. radius footprint. In this figure, the increase in deflection due to cracking is indicated by the difference between the curves of measured deflection and the dashed line representing an extrapolation of the deflection for the condition of no cracking in the slab. The deflections measured for Slab No. 1 and Slab No. 5 represent the effects of two different types of

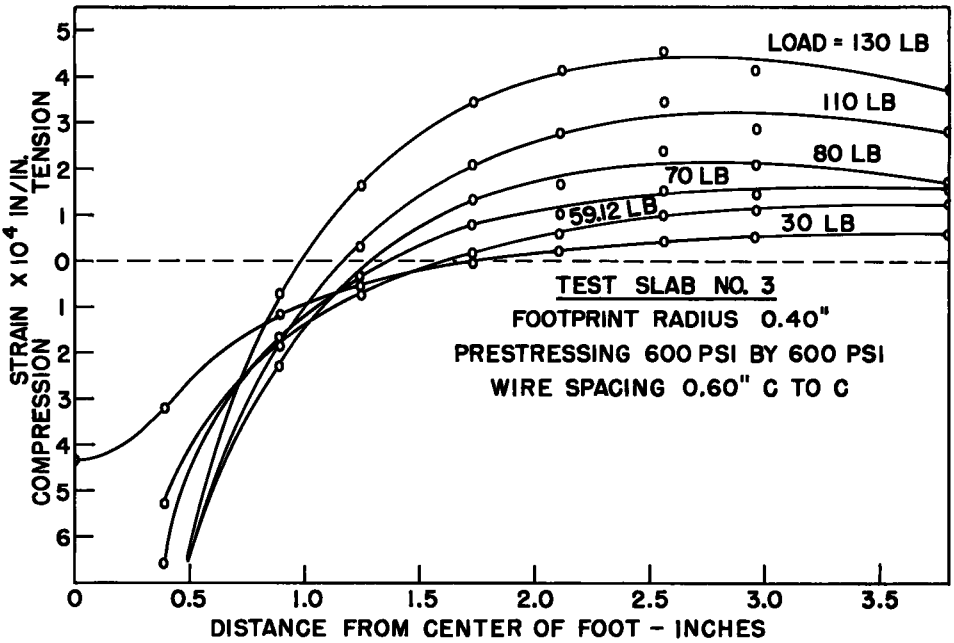

Figure 18. Distribution of radial strains in surface of model slab for interior loadings beyond elastic range.

cracking (see Figs. 8 and 9). Compared to the two prestressed slabs, the somewhat larger deflections measured in the plain slab indicated that the stressing wires had appreciable ability to reduce the deflection for loadings beyond the elastic range.

Strain Distribution

During the early stages of the model studies, an effort was made to determine what the positioning of the SR-4 gages relative to the stressing wires might have on the indicated strains. In these tests, various combinations of strain gage - stressing wire orientation were investigated. Typical of the results obtained are those shown in Figure 16 for loadings on Slab No. 3. By cementing a line of gages to the top side of the slab so that the gages were positioned alternately over the intersection of two stressing wires and between the stressing wires, it was possible to develop strain distribution curves for each gage orientation. In this case, the gages positioned directly over the wires indicated strains approximately 5 percent greater than did the gages located between the wires. Tests on other gages failed to indicate effects due to orientation greater than plus or minus 5 percent of the measured strains. Consequently, it was decided to omit any corrections for gage orientation and, wherever possible, to center the gages and footprints over wire intersections.

For loadings producing critical stresses within the elastic limit of the slab, the

distribution of strain in the slab around the loaded area was found to be similar to that for a plain slab. Curves showing the distribution of radial strain for a 25-lb loading on various sizes of circular footprints are presented in Figure 17. These curves indicate that footprint size has little or no effect on strains beyond the contact area of the footprint for radii of 0.75-in. and smaller. The lack of conformity shown by the 1.50-in. radius foot suggests that the slab did not perform as though infinite in horizontal extent for a footprint of that size.

For loadings producing critical stresses behond the elastic limit of the slab, the distribution of strain was found to be a function of the magnitude of the loading. Figure 18 shows the distribution of radial strains in the surface of Slab No. 3 for various loadings on an 0.4-in. radius circular footprint. The curve for the 30-lb loading represents the distribution for elastic behavior of the slab. The curves for loadings greater than 30 lb represent conditions in which cracking existed in the bottom side of the slab, the

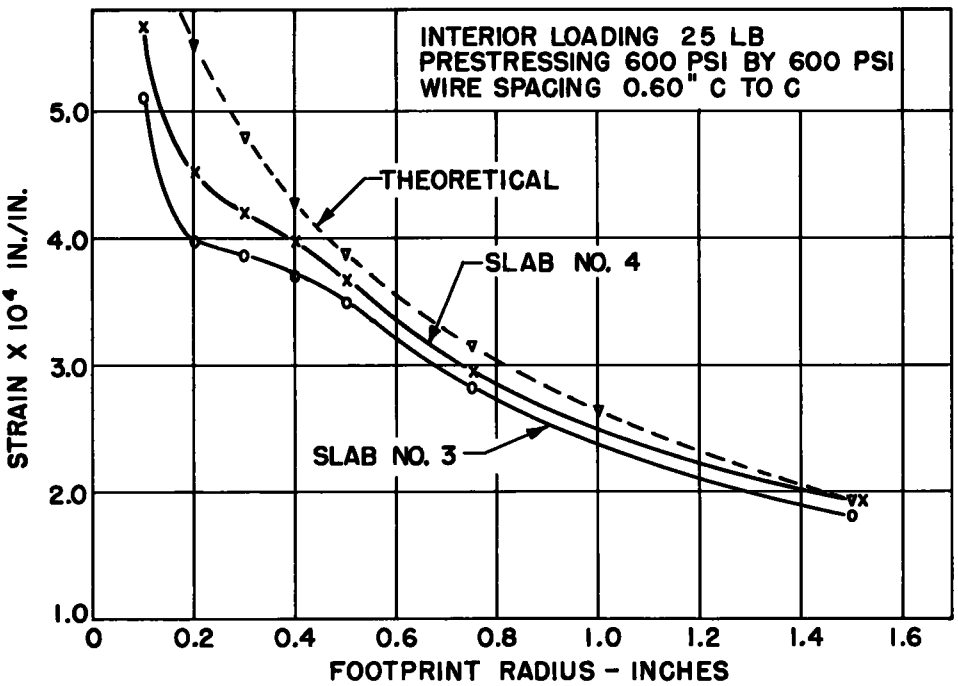

Figure 19. Effect of footprint size on maximum strain for interior loadings within the elastic range.

degree of cracking increasing with increasing load as shown previously. It can be seen from this figure that as the load was increased, both the point of maximum strain and the point of zero strain in the top of the slab moved toward the center of loading. The loading was discontinued at 130 lb when it became apparent that cracking in the top of the slab would not occur prior to complete failure of the slab at approximately 150 to 160 lb. On the basis of the strains measured in Slab No. 3, it was estimated that the maximum negative strain in the top of the slab for an ultimate load of 160 lb would be approximately 75 percent of the strain required to produce cracking.

Maximum Strains

In comparing maximum strains versus footprint radius for loadings within the elastic limit, certain sizes of footprints indicated a tendency to deviate from the relationship obtained with plain slabs. In Figure 19, curves of maximum strain versus footprint radius are shown for two different test slabs for comparison with the curve as given by the Westergaard analyses. In previous testing with plain slabs, it has been shown

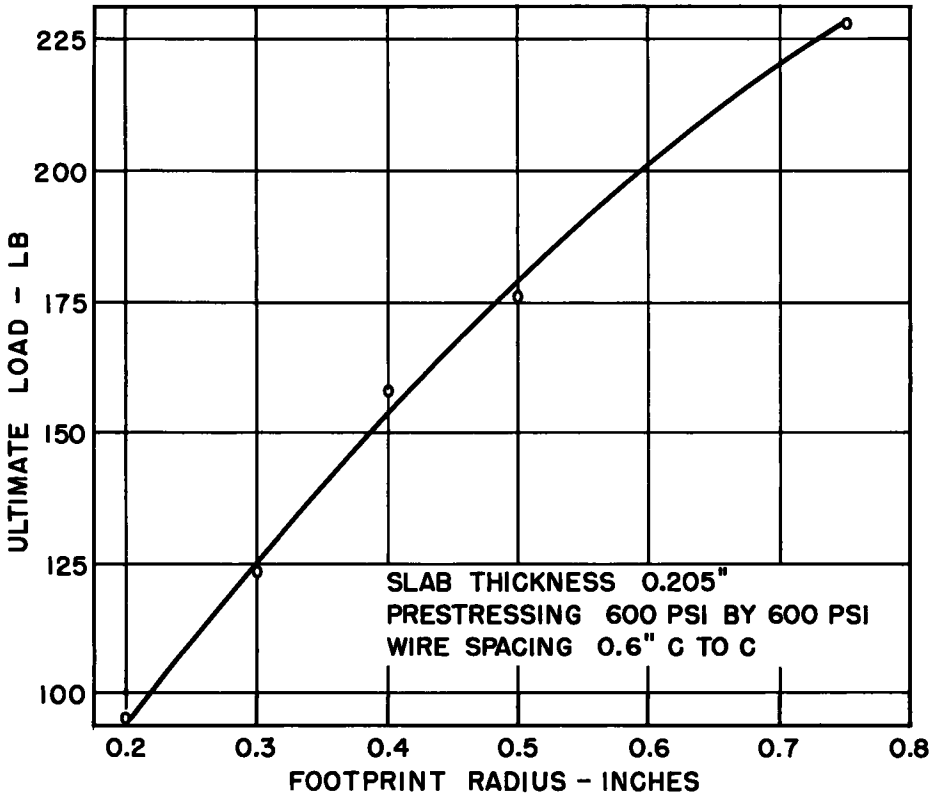

Figure 20. Effect of footprint size on ultimate load for interior loadings.

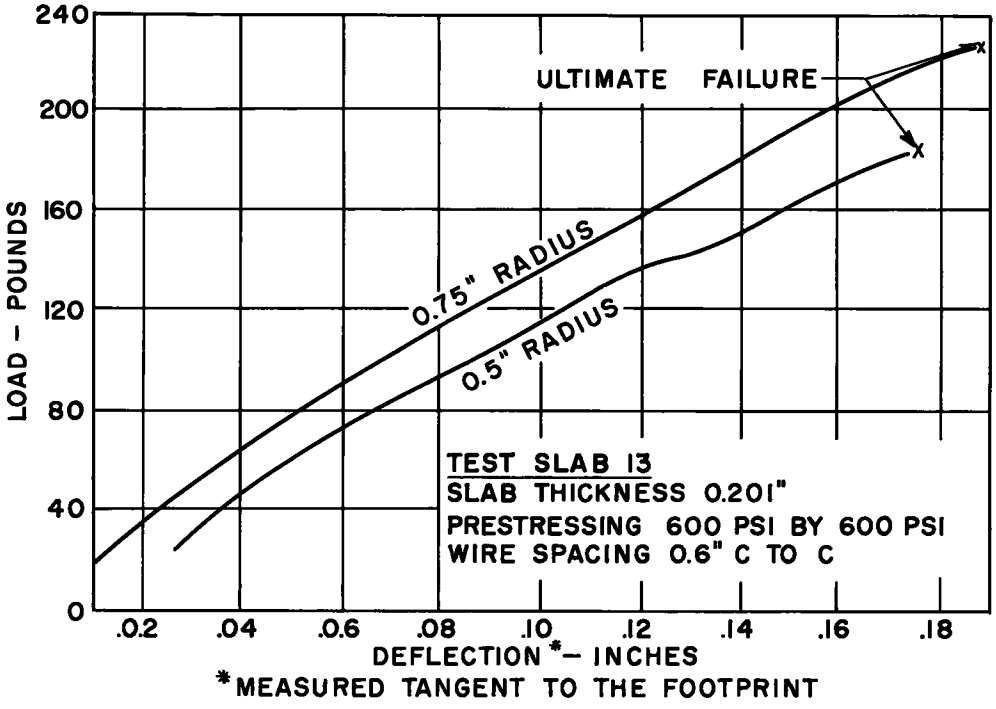

Figure 21. Deflection curves for interior loadings to ultimate failure.

that data obtained from the model closely paralleled the theory. In Figure 19, however, it is evident that the 0.2-, 0.3- and 0.4-in. radius footprints gave lower than normal values for the maximum strain. Although no definite reason for this deviation could be determined, it was believed to be related to the spacing of the stressing wires.

Ultimate Loading

In the testing completed to date, several of the model slabs have been loaded to complete failure. By using various sizes of footprints, the relationship between footprint size and ultimate load was developed, as shown in Figure 20, for model slabs having equal prestressing of 600 psi longitudinally and transversely. In the model tests, the failures were always characterized by the footprint punching through the slab and into the subgrade. Load-deflection curves for 0.50- and 0.75-in. radius footprints are shown in Figure 21 for ultimate load tests on Slab No. 13. Maximum deflections at incipient failure approximated 90 percent of the slab thickness.

A comparison of loads producing initial cracking and ultimate failure for both plain slabs and slabs prestressed to 600 psi longitudinally and transversely are presented in Table 3. Ultimate failure in these tests, defined as the load at which the footprint punched through the slab, does not necessarily represent failure in the prototype. However, these data afford some measure of the relative load-carrying capacities of prestressed pavements as compared to plain rigid pavements. In addition to the advantage of greater load-carrying capacity gained through the use of prestressing, it should be pointed out that for the design of airfield pavements prestressing will permit criteria based on the less severe interior loading as compared to the present criteria based on edge loading of plain rigid pavements.

SUMMARY OF FINDINGS

1. For pretensioning, the full amount of prestress was developed over a period of 36 to 48 hr rather than immediately following the release of the stressing wires.
2. For stressing wires placed at mid-depth in the slab and for loadings within the elastic range, prestressing had no effect on the structural rigidity of the slab. Measured strains and deflections were similar in both plain and prestressed slabs for comparable loadings.
3. Prestressing permitted the slabs to sustain greater loads prior to initial cracking for both edge and interior loadings.
4. Prestressed slabs maintained a substantial portion of their structural integrity following loadings beyond the range of elastic behavior.
5. Initial cracking occurred in a radial pattern originating in the bottom side of the slab and under the center of the loaded area.
6. Prior to complete failure, cracking was confined to the bottom side of the prestressed slabs.
7. Crack patterns were dependent upon both the manner of loading and the spacing of the stressing wires, and were not effected significantly by the magnitude of the prestressing.
8. Independent cracking occurred for loads spaced at intervals of not less than one footprint diameter.
9. Footprint size had little effect on deflections beyond the loaded area for both elastic and inelastic conditions of loading.
10. For loadings beyond the elastic range, greater deflections were observed in the plain slabs than in prestressed slabs subjected to the same loading.
11. Prestressed slabs were capable of sustaining greater deflections prior to ultimate failure than were the plain slabs.
12. For loadings beyond the elastic range, the point of maximum negative strain in the surface of a prestressed slab moved toward the center of the loaded area as the load was increased.
13. For loadings beyond the elastic range, negative strains in the surface of a prestressed slab increased at a greater rate than the loads producing the strains.

CONCLUSIONS

These studies have shown that small scale models of prestressed rigid pavements can be constructed successfully, and that these slabs, when subjected to controlled static loadings, exhibit characteristics believed to be analogous to those of the prototype. Therefore, it is concluded that this type of testing can be a useful and valid tool for investigating the behavior of prestressed airfield pavements for various conditions of loading and prestressing.

Since the construction and testing of the models is continuing, much of the data presented herein are incomplete. It is hoped that further study now programmed will contribute to the present knowledge of prestressed pavements.

ACKNOWLEDGMENTS

The studies reported in this paper were made by the Research Branch of the Ohio River Division Laboratories, as a part of the Corps of Engineers, U.S. Army, Rigid Pavement Investigational Program. This program is directed and coordinated by the Airfields Branch, Engineering Division for Military Construction, Office, Chief of Engineers. This work was done under and by the authority of the Chief of Engineers, U.S. Army.

REFERENCES

1. Mellinger, F.M. and Carlton, P.F., "Application of Models to Design Studies of Concrete Airfield Pavements," Proc., Highway Research Board, Vol. 34, 1955.

2. Carlton, P.F. and Behrmann, Ruth M., "A Model Study of Rigid Pavement Behavior under Corner and Edge Loadings," Proc., Highway Research Board, Vol. 35, 1956.

3. Westergaard, H.M., "Stresses in Concrete Pavements Computed by Theoretical Analysis," Public Roads, April 1926.

4. Westergaard, H.M., "Stress Concentrations in Plates Loaded Over Small Areas," Transactions, Am. Soc. of Civil Eng., Vol. 108, 1943.

5. Westergaard, H.M., "New Formulas for Stresses in Concrete Pavements of Airfields," Trans., Am. Soc. of Civil Eng., Vol. 113, 1947.